NANO LETTERS

2008
Vol. 8, No. 4
1163-1168

Directing the Assembly of Charged Organic Molecules by a Hydrophilic−Hydrophobic Nanostructured Monolayer at Electrified Interfaces

Andrey S. Klymchenko,*,†,‡ Shuhei Furukawa,†,|| Mark Van der Auweraer,† Klaus Müllen,§ and Steven De Feyter*,†

Department of Chemistry, Laboratory of Photochemistry and Spectroscopy, and Institute of Nanoscale Physics and Chemistry (INPAC), Katholieke Universiteit Leuven, Celestijnenlaan 200-F, 3001 Leuven, Belgium, Department of Pharmacology and Physical Chemistry, UMR 7175, Institut Gilbert Laustriat, Université Louis Pasteur (Strasbourg I), BP 60024, 67401 Illkirch, France, and Max-Planck-Institut für Polymerforschung, Ackermannweg 10, D-55021 Mainz, Germany

Received December 21, 2007; Revised Manuscript Received February 7, 2008

ABSTRACT

Nanostructured monolayers of water-insoluble amphiphilic 5-alkoxy-isophthalic acids direct the reversible self-assembly of water-soluble positively and negatively charged molecules under electrochemical control. The surface potential is in control of the monolayer composition, structure, and guest dynamics.

Introduction. Supramolecular organization in two dimensions is the subject of intensive research because it potentially allows the formation of functional surfaces, including the development of prototypes of future molecule-based electronic devices.[1] Supramolecular structures realized to date include clusters, chains, and extended 2D networks. One of the main challenges is the generation of multicomponent highly organized supramolecular nanostructures in a well-controlled manner.

Mainly, bicomponent systems have been targeted[2] and a number of different approaches can be distinguished: **Type 1**. Mixing of the molecular components gives rise to the formation of a completely new type of ordering, in no way reflecting the organization of (one of) the pure components. Basically, a 2D cocrystal is formed.[3–7] **Type 2**. Mixing leads to a new type of ordering, which at least resembles (or is identical to) the self-assembly pattern of one (or both of) the pure components. Typically, one of the components forms a 2D supramolecular host network, which then allows epitaxial coassembly of the molecules of interest[8–24] **Type 3**. Guest molecules adsorb *on top of* the host template.[25–29]

Typically, multicomponent systems have been created under UHV conditions or at "classical" solid–liquid and solid−air interfaces. Electrified interfaces, though, have one major advantage: molecule−substrate interactions can be readily controlled by an external parameter, the substrate potential. Recently we showed by electrochemical scanning tunneling microscopy[30–35] the self-assembly of amphiphilic 5-hexadecyloxy-isophthalic acid (ISA16) into uncharged hydrophobic−hydrophilic nanopatterns at an electrified interfaces (Figure 1A).[36] We envisioned a unique approach to controlled coassembly of multicomponent systems on surfaces: the use of a noncharged water-insoluble amphiphile to form hydrophobic−hydrophilic nanostructured surfaces for the directed adsorption of water-soluble polar charged molecules.

* Corresponding authors. E-mail: Steven.DeFeyter@chem.kuleuven.be (S.D.); aklymchenko@pharma.u-strasbg.fr (A.K.). Telephone: +32 16 327921 (S.D.); +33 390244255 (A.K.). Fax: +32 16 327990 (S.D.).

† Department of Chemistry, Laboratory of Photochemistry and Spectroscopy, and Institute of Nanoscale Physics and Chemistry (INPAC), Katholieke Universiteit Leuven.

‡ Department of Pharmacology and Physical Chemistry, UMR 7175, Institut Gilbert Laustriat, Université Louis Pasteur (Strasbourg I).

§ Max-Planck-Institut für Polymerforschung.

|| Present address: ERATO Kitagawa Integrated Pores Project, Japan Science and Technology Agency (JST), Kyoto Research Park Bldg 3, Shimogyo-ku, Kyoto 600-8813, Japan.

10.1021/nl073352d CCC: $40.75
Published on Web 03/01/2008

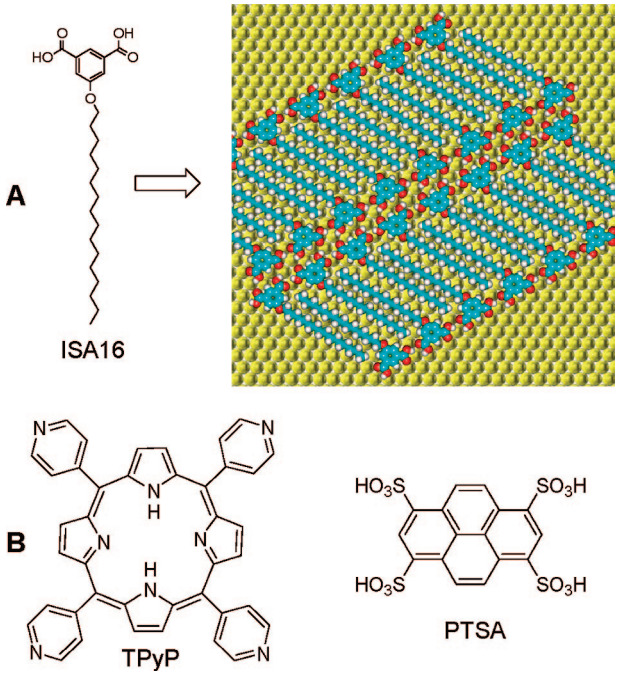

Figure 1. (A) Schematic presentation of the self-assembly of ISA16 into hydrophobic−hydrophilic nanopatterns on Au(111).[36] Hydrophilic regions are formed by the isophthalic acid moieties and hydrophobic regions by the alkyl chains of ISA16. (B) Chemical structures of TPyP and PTSA.

In this contribution, the first examples of this concept are reported: coassembly of 5,10,15,20-tetra(4-pyridyl)-21H,23H-porphine (TPyP) and pyrene tetrasulfonic acid (PTSA) (Figure 1B), which at pH 1 (0.1 M $HClO_4$ electrolyte) are positively and negatively charged ions, respectively, within nanostructured monolayers of neutral and water-insoluble ISA16 (Figure 1A). TPyP forms disordered domains that are separated by individual lamellae of ISA16. In sharp contrast, PTSA forms mono- or bimolecular chains assembled in the hydrophilic grooves of ISA16 lamellae. This higher degree of order is attributed to the good match between the structural parameters of the PTSA molecule and the ISA16 lattice.

An important advantage of this approach is that the coassembly depends on the surface potential. The nanostructured surface formed by the water-insoluble molecules is confined to the substrate for a broad potential window, while the guest molecules are expected to show a stronger response (adsorption/desorption/in-plane mobility) to changes in the applied potential, as will be illustrated. Thus, the surface composition, structure, and dynamics can be controlled by the potential, in a reversible way.

Results and Discussion. First, we discuss shortly the self-assembly of the water-soluble guest molecules and then focus on their coassembly within the ISA16 matrix.

Self-Assembly of the Water-Soluble Guest Molecules on Au(111). ***TPyP.*** An STM image of a self-assembled monolayer of TPyP at the interface between Au(111) and 0.1 M $HClO_4$ solution is presented in Figure 2.

At these pH conditions, the porphyrins are protonated. The selected electrode (substrate) potential (400 mV SCE) is close to the potential of zero charge, where ISA16 molecules are

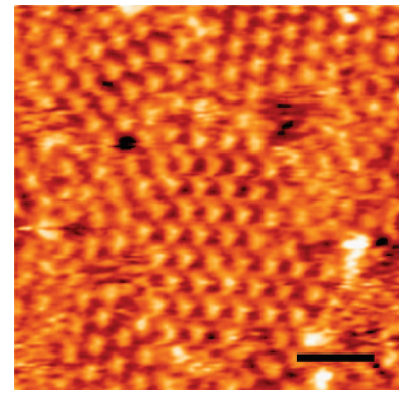

Figure 2. STM images of TPyP on Au(111) in 0.1 M $HClO_4$. Electrode (substrate) potential, E_w = 400 mV (vs SCE). Bias voltage, U_{bias} = –500 mV. Tunneling current, I_t = 1 nA. Scale bar is 4.3 nm.

expected to form a parallel arrangement of stable lamellae.[36] At this substrate potential, porphyrin molecules are observed as bright features forming a hexagonal supramolecular arrangement in relatively small domains, which are oriented parallel or at an angle of ca. 20° with respect to each other. Previous studies of TPyP in 0.1 M H_2SO_4 electrolyte showed a square 2D lattice.[37] The differences in the molecular ordering observed in these two different electrolytes are attributed to the influence of the anions in the TPyP packing on Au(111). We speculate that the observed square arrangement in H_2SO_4 is due to the participation of sulfate anions in the TPyP packing, which, in contrast to perchlorate anions, may form strongly adsorbed ordered monolayers at the Au(111)–electrolyte interface.[38] The distance between TPyP molecules in the lattice observed in 0.1 M $HClO_4$ is ca. 1.6 nm, the size of the molecule, estimated as the distance between nearest pyridine nitrogen atoms is 1.1 nm. Thus, the observed intermolecular distance in the TPyP hexagonal lattice (1.6 nm) does not match the distance between adjacent isophthalic acid groups along the ISA16 lamellae (ca. 1.0 nm).[36]

PTSA. PTSA molecules added to the electrolyte−Au(111) interface at positive electrode potentials arrange in linear patterns with zigzag-like distortions (Figure 3). PTSA being a strong acid, is negatively charged at pH 1 due to deprotonation of the sulfonate groups in contrast to TPyP. The formation of the linear structures is in line with the 2-fold symmetry of PTSA. The distance between PTSA molecules inside the rows measures $a = 0.95 \pm 0.05$ nm (Figure 3B). Importantly, this distance perfectly matches the spacing of the isophthalic acid groups in ISA16 lamellae, which will have a clear effect on the structure of the PTSA/ISA16 mixtures (vide infra).[36] The nearest distance between molecules in neighboring molecular rows, b, is slightly larger: 1.30 ± 0.05 nm. Moreover, according to the obtained STM images, the long molecular axes appear tilted with respect to the molecular row normal by $\alpha = 25 \pm 5°$ (Figure 3B). This tilt is expected to optimize the dense packing of the negatively charged sulfonate groups at the interface (Figure 3C).

Coassembly with ISA16 Lamellae. In the next step, coassembly of the oppositely charged guest molecules with

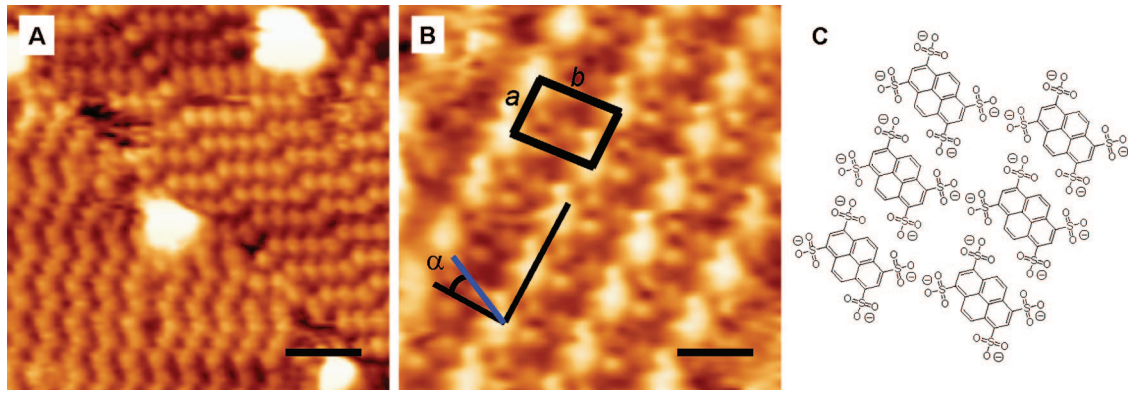

Figure 3. (A,B) STM images of PTSA on Au(111) in 0.1 M $HClO_4$. $E_w = 500$ mV (vs SCE). $U_{bias} = -500$ mV. $I_t = 1$ nA. Scale bars are 3.9 nm (A) and 1.2 nm (B). Unit cell is shown in B. The blue line is the orientation of the long molecular axes of the PTSA molecules at an angle α with respect to the molecular row normal. (C) Tentative schematic presentation of packing of PTSA on Au(111).

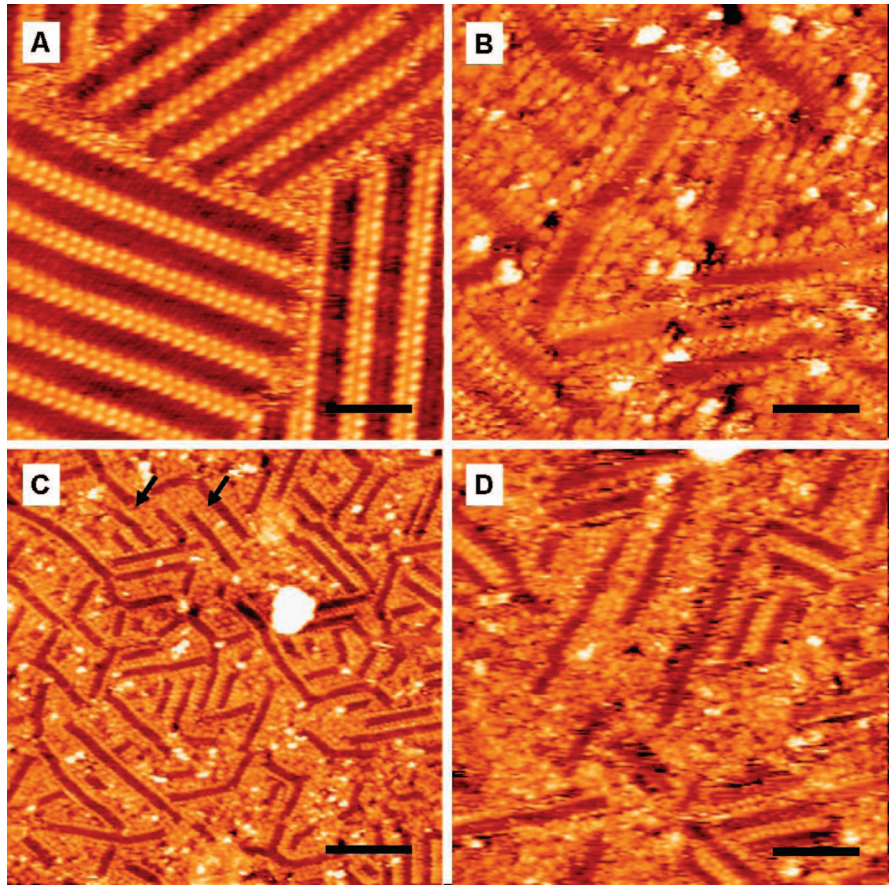

Figure 4. STM images of a hydrophobic−hydrophilic nanostructured monolayers formed by ISA16 in absence (A) and in presence of 1 μM of TPyP (B,C, and D). (A) $E_w = 300$ mV (vs SCE), $U_{bias} = -200$ mV, $I_t = 1$ nA. (B,C) $E_w = 250$ mV (vs SCE), $U_{bias} = -260$ mV, $I_t = 1$ nA. (D) $E_w = 500$ mV (vs SCE), $U_{bias} = -450$ mV, $I_t = 1$ nA. The high positive electrode potential leads to an increased mobility of the TPyP molecules. The scale bars are 5.8 nm (A,B), 14 nm (C), and 8.6 nm (D).

the hydrophilic−hydrophobic ISA16 nanostructured monolayers was targeted and potential dependent dynamics were probed.

TPyP and ISA16. To coassemble TPyP molecules within the ISA16 template, first, ISA16 monolayers were prepared as described previously (Figure 4A).[36] Then a solution of TPyP in 0.1 M $HClO_4$ was added directly to the liquid cell of the electrochemical STM at a substrate potential of 250 mV (vs SCE). On addition of TPyP, one observes the formation of a mixed phase containing both molecules (Figure 4B,C). The formation of the mixed phase of ISA16 and TPyP is a relatively slow process. Only after approximately 1 h, the formation of the mixed phase is completed. ISA16 nanopatterns are split into individual lamellae and the TPyP molecules form disordered domains ("pools") between ISA16 lamellae (Figure 4). Individual ISA16 lamellae were previously observed for pure ISA16 monolayers at potentials around 500 mV.[36] In the presence of TPyP, the individual lamellae of ISA16 are observed at much lower potentials, which must be attributed to the

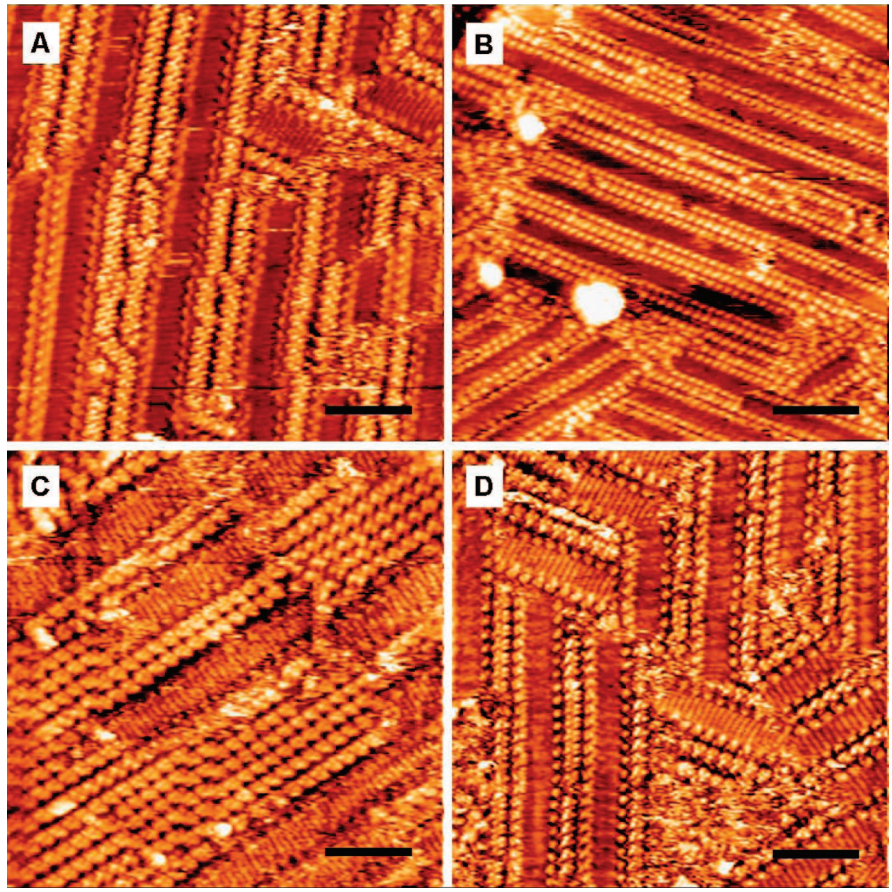

Figure 5. Assembly of PTSA molecules within the lamella template of ISA16 in 0.1 M $HClO_4$ on Au(111) at different electrode potentials. (A) $E_w = 400$ mV, $U_{bias} = -240$ mV, $I_t = 1$ nA. (B) $E_w = 350$ mV, $U_{bias} = -330$ mV, $I_t = 1$ nA. (C) $E_w = 700$ mV, $U_{bias} = -650$ mV, $I_t = 1$ nA. (D) After potential jump from $E_w = 1000$ mV (where only PTSA observed) to 400 mV, $U_{bias} = -325$ mV, $I_t = 1$ nA. Scale bars are 5.8 nm (A,C,D) and 8.8 nm (B).

adsorption of TPyP molecules on the electrode surface. The ISA16 lamellae do not run straight because their arrangement is perturbed by the adsorbed TPyP molecules. The lack of order in the TPyP domains is due to the poor commensurability of the TPyP hexagonal lattice (Figure 2) with the ISA16 matrix. The TPyP molecules adjacent to the ISA16 lamellae are well-resolved though, indicating that they are immobilized. The protonated pyridine groups may form H-bonds with the carboxyl groups of the ISA16 molecules. However, the spacing between TPyP molecules is significantly larger than the spacing between isophthalic acid groups within the lamellae. This lack in structural match impedes the formation of a highly ordered coassembly. Single molecular rows of TPyP between ISA16 lamellae were observed though (Figure 4C).

Variation of the substrate potential does not modify significantly the molecular arrangement of the mixed phase. However, at more positive potentials (ca. 500 mV), the bright spots corresponding to the TPyP molecules are no more detectable (Figure 4D). This observation can be explained by an increase in the mobility of the positively charged TPyP molecules, which at the more positive substrate potentials should show a lower affinity to the Au(111) surface.

PTSA and ISA16. As the structural parameters of PTSA assembly match those of ISA16 much better, a complementary type of coassembly was anticipated. A PTSA solution was added after formation of a ISA16 template layer at the appropriate substrate potential (350 mV vs SCE). ISA16 molecules are again observed to order in individual lamellae. Bright features appeared between the ISA16 lamellae (Figure 5A,B). These bright features showing a four-lobe structure can be unambiguously assigned to the PTSA molecules assembling between the ISA16 lamellae. In the separate PTSA domains, the molecules run parallel to ISA16 lamellae (Figure 5C), which corresponds to the next-nearest-neighborhood (NNN) direction of Au(111). This particular orientation of the PTSA molecular rows is favored by molecule−substrate interactions because the spacing between the PTSA molecules (and the length of the molecule measured as the distance between 1- and 6-sulfonate groups) corresponds well to the double distance between gold atoms along the NNN direction (ca. 1 nm). In addition to PTSA domains, remarkably enough, one observed the formation of both mono- and bimolecular rows of PTSA. The spacing between PTSA molecules in these molecular rows measures 0.95 ± 0.05 nm, which perfectly matches the spacing between the ISA16 aromatic residues in the lamellae. Thus, both the orientation of rows of PTSA molecules and their intermolecular spacing are commensurate with the orientation of the isophthalic acid moieties of ISA16 and their spacing within the lamellae, allowing a tight packing. In addition, PTSA molecules are rotated with respect to the molecular row normal, although

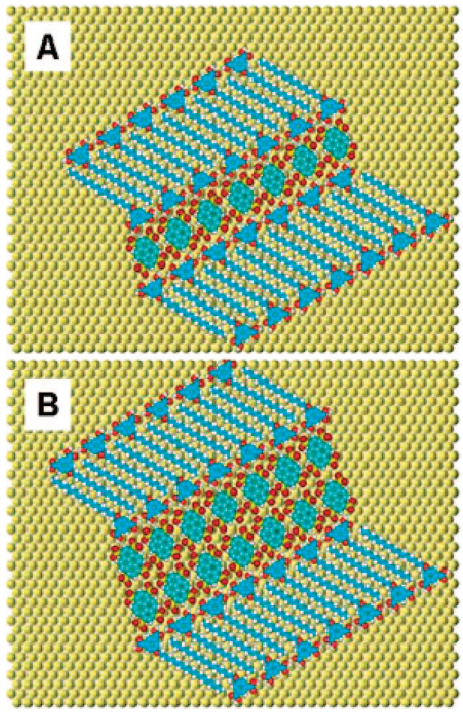

Figure 6. Models of the ordering of PTSA molecules in the ISA16 template on Au(111). Single (A) and double (B) molecular chains are presented.

this tilt angle is significantly smaller, namely $\alpha = 10 \pm 5°$ (Figures 3B and 5), compared to pure PTSA monolayers. This is explained by the interaction of PTSA with the isophthalic acid moieties, which partially compensates the repulsive forces between the negatively charged sulfonate groups. A tentative model of the supramolecular arrangement of PTSA molecules inside the ISA16 matrix (Figure 6A,B) clearly illustrates the complementary coassembly of monomolecular and bimolecular rows PTSA rows in between isophthalic acid rows.

At more positive potentials, an increase in the fraction of adsorbed PTSA molecules is observed that is explained in terms of the increased affinity of the negatively charged PTSA molecules to the Au(111) substrate. The PTSA molecules appear in ordered small domains with a similar organization as for the pure system (Figures 5C). However, almost no zigzag distortions, typical for pure PTSA monolayers (Figure 3A), are observed in this case, indicating the key role of the ISA16 matrix in aligning PTSA molecular rows.

At highly positive potentials (ca. 1000 mV), PTSA molecules were observed exclusively (same arrangement as shown in Figure 3 and 5C). By tuning the potential, one can therefore control the surface composition and supramolecular organization. Remarkably, after a work potential jump from 1000 to 400 mV, the recovery of the ordered mixed phase is observed: PTSA molecules form molecular rows between ISA16 lamellae (Figure 5D). Thus, the formation of the molecular rows of PTSA molecules within the ISA16 template is a reversible process.

The present results confirm that the ISA16 assembly is a hierarchical process: the primary step of their assembly is the formation of interdigitated lamellae stabilized by hydrophobic van der Waals interactions between the hydrocarbon chains, by hydrogen bonding interactions along the row axis, and by the molecule−substrate interactions. The interaction between adjacent lamellae is relatively weak. Therefore, this polar region between lamellae can be disrupted easily by the adsorption of charged molecules at appropriate substrate potentials.

How to explain then the difference between TPyP and PTSA coassembly with ISA16? PTSA, unlike TPyP, forms mono- and bimolecular rows between the carboxylic boundaries of the ISA16 lamellae for the following reasons: (1) the perfect match of the spacing between PTSA molecules and ISA residues in the lamellae, (2) perfect match of the direction of the molecular rows of PTSA with the ISA16 lamellae direction, and (3) 2-fold symmetry of PTSA molecules that favors the formation of molecular rows (1D nanostructures) rather than 2D hexagonal or square arrangements. These can be considered as general guidelines to direct the coadsorption of guest molecules.

In conclusion, the successful use of water-insoluble neutral hydrophobic−hydrophilic nanostructured monolayers to direct the ordering of water-soluble charged organic guest molecules at electrified interfaces is demonstrated. Both negatively and positively charged guest molecules adsorb in between the hydrophilic regions of the nanostructured surface. Not surprisingly, a structural match between the guest molecules and the host lamellar matrix is crucial in order to achieve a high degree of order. Unlike TPyP that forms disordered domains, PTSA forms highly ordered mono- and bimolecular rows in the ISA16 matrix. In addition, the composition of the multicomponent pattern can be tuned reversibly by adjusting the substrate potential. These insights pave the way to the realization of more complex and functional nanostructures at electrified interfaces.

Acknowledgment. We thank the Belgian Federal Science Policy through IAP 6/27, the Fund for Scientific Research—Flanders (FWO), Fondation pour la Recherche Médicale (FRM), Program Tournesol, and Marie-Curie RTN "Chextan". A.K. thanks FWO for financial support. S.F. is grateful to the JSPS Postdoctoral Fellowships for Research Abroad and the Murata Science Foundation. We thank KU Leuven and BelSpo for financial support through GOA 2006/2 and the German Science Foundation (FFB/TRR 49). Prof. Charl Faul is acknowledged for providing a sample of PTSA.

Supporting Information Available: Experimental details. This material is available free of charge via the Internet at http://pubs.acs.org.

References

(1) Jackel, F.; Watson, D.; Müllen, K.; Rabe, J. P. *Phys. Rev. Lett.* **2004**, *92*, 188383.
(2) Yang, Y. L.; Wang, C. *Int. J. Nanotechnol.* **2007**, *4*, 1–20.
(3) Hipps, K. W.; Scudiero, L.; Barlow, D. E.; Cooke, M. P., Jr. *J. Am. Chem. Soc.* **2002**, *124*, 2126–2127.
(4) Nath, K. G.; Ivasenko, O.; Miwa, J. A.; Dang, H.; Wuest, J. D.; Nanci, A.; Perepichka, D. F.; Rosei, F. *J. Am. Chem. Soc.* **2006**, *128*, 4212–4213.
(5) De Feyter, S.; Miura, A.; Yao, S.; Chen, Z.; Würthner, F.; Jonkheijm, P.; Schenning, A. P. H. J.; Meijer, E. W.; De Schryver, F. C. *Nano*

Lett. **2005**, *5*, 77–81.
(6) Canas-Ventura, M. E.; Xiao, W.; Waserfallen, D.; Müllen, K.; Brune, H.; Barth, J. V.; Fasel, R. *Angew. Chem., Int. Ed.* **2007**, *46*, 1814–1818.
(7) Stepanow, D.; Lin, N.; Payer, D.; Schlickum, U.; Klappenberger, F.; Zoppellaro, G.; Ruben, M.; Brune, H.; Barth, J. V.; Kern, K. *Angew. Chem., Int. Ed.* **2007**, *46*, 710–713.
(8) Eichhorst-Gemer, K.; Stabel, A.; Moessner, G.; Declerq, D.; Valiyaveettil, S.; Enkelmann, V.; Müllen, K.; Rabe, J. P. *Angew. Chem., Int. Ed. Engl.* **1996**, *35*, 1492–1495.
(9) Lei, S. B.; Wang, C.; Yin, S. X.; Bai, C. L. *J. Phys. Chem.* **2001**, *105*, 12272–12277.
(10) Vanoppen, P.; Grim, P. C. M.; Rücker, M.; De Feyter, S.; Moessner, G.; Valiyaveetil, S.; Müllen, K.; De Schryver, F. C. *J. Phys. Chem.* **1996**, *100*, 19636–19641.
(11) Gesquière, A.; Abdel-Mottaleb, M. M.; De Feyter, S.; De Schryver, F. C.; Sieffert, M.; Müllen, K.; Calderone, A.; Lazzaroni, R.; Brédas, J.-L. *Chem.—Eur. J.* **2000**, *6*, 3739–3746.
(12) Mena-Osteritz, E.; Bauërle, P. *Adv. Mater.* **2006**, *18*, 447.
(13) Pan, G. B.; Cheng, X. H.; Höger, S.; Freyland, W. *J. Am. Chem. Soc.* **2006**, *128*, 4218–4219.
(14) Safarowsky, C.; Merz, L.; Rang, A.; Broekmann, P.; Hermann, B. A.; Schalley, C. A. *Angew. Chem., Int. Ed.* **2004**, *43*, 1291–1294.
(15) Theobald, J. A.; Oxtoby, N. S.; Phillips, M. A.; Champness, N. R.; Beton, P. H. *Nature* **2003**, *424*, 1029–1031.
(16) Wintjes, N.; Bonifazi, D.; Cheng, F.; Kiebele, A.; Stöhr, M.; Jung, T.; Spillman, H.; Diederich, F. *Angew. Chem., Int. Ed.* **2007**, *46*, 4089–4092.
(17) Gong, J.-R.; Yan, H.-J.; Yuan, Q.-H.; Xu, L.-P.; Bo, Z.-S.; Wan, L.-J. *J. Am. Chem. Soc.* **2006**, *128*, 12384–12385.
(18) Lu, J.; Lei, S.-B.; Zeng, Q.-D.; Kang, S.-Z.; Wang, C.; Wan, L.-J.; Bai, C.-L. *J. Phys. Chem. B* **2004**, *108*, 5161–5165.
(19) Furukawa, S.; Tahara, K.; De Schryver, F. C.; Van der Auweraer, M.; Tobe, Y.; De Feyter, S. *Angew. Chem., Int. Ed.* **2007**, *46*, 2831–2834.
(20) Schull, G.; Douillard, L.; Fiorini-Debuisschert, C.; Charra, F.; Mathevet, F.; Kreher, D.; Attias, A.-J. *Nano. Lett.* **2006**, *6*, 1360–1363.
(21) Pan, G. B.; Liu, M.; Zhang, H. M.; Wan, L. J.; Zheng, Q. Y.; Bai, C. L. *Angew. Chem., Int. Ed.* **2003**, *42*, 2747–2751.
(22) Yoshimoto, S.; Sugawara, S.; Itaya, K. *Electrochemistry* **2006**, *74*, 175–178.
(23) Yoshimoto, S.; Tsutsumi, E.; Fujii, O.; Narita, R.; Itaya, K. *Chem. Commun.* **2005**, 1188–1190.
(24) Yoshimoto, S.; Higa, N.; Itaya, K. *J. Am. Chem. Soc.* **2004**, *126*, 8540–8545.
(25) Yang, Z. Y.; Gan, L. H.; Lei, S. B.; Wan, L. J.; Wang, C.; Jiang, J. Z. *J. Phys. Chem. B* **2005**, *109*, 19859–19865.
(26) Piot, L.; Marchenko, A.; Wu, J. S.; Müllen, K.; Fichou, D. *J. Am. Chem. Soc.* **2005**, *127*, 16245–16250.
(27) Safarowsky, C.; Rang, A.; Schalley, C. A.; Wandelt, K.; Broekmann, P. *Electrochim. Acta* **2005**, *50*, 4257–4268.
(28) Safarowsky, C.; Wandelt, K.; Broekmann, P. *Langmuir* **2004**, *20*, 8261–8269.
(29) Yoshimoto, S.; Tsutsumi, E.; Narita, R.; Murata, Y.; Murata, M.; Fujiwara, K.; Komatsu, K.; Ito, O.; Itaya, K. J. *Am. Chem. Soc.* **2007**, *129*, 4366–4376.
(30) Itaya, K. *Prog. Surf. Sci.* **1998**, *58*, 121–247.
(31) Kolb, D. M. *Surf. Sci.* **2002**, *500*, 722–740.
(32) He, Y.; Ye, T.; Borguet, E. *J. Am. Chem. Soc.* **2002**, *124*, 11964–11970.
(33) Safarowsky, C.; Merz, L.; Rang, A.; Broekmann, P.; Hermann, B. A.; Schalley, C. A. *Angew. Chem., Int. Ed.* **2004**, *43*, 1291–1294.
(34) Yashimoto, S. *Bull. Chem. Soc. Jpn.* **2006**, *79*, 1167–1190.
(35) Wang, D.; Wan, L.-J. *J. Phys. Chem. C* **2007**, *111*, 16109–16130.
(36) Klymchenko, A. S.; Furukawa, S.; Müllen, K.; Van der Auweraer, M.; De Feyter, S. *Nano Lett.* **2007**, *7*, 791–795.
(37) He, Y.; Ye, T.; Borguet, E. *J. Am. Chem. Soc.* **2002**, *124*, 11964–11970.
(38) Magnussen, O. M. *Chem. Rev.* **2002**, *102*, 679–726.

NL073352D